BLADE OBLIQUE CUTTING OF TISSUE FOR INVESTIGATION OF BIOPSY NEEDLE INSERTION

Jason Z. Moore and Albert J. Shih
Department of Mechanical Engineering
University of Michigan
Ann Arbor, Michigan

Patrick W. McLaughlin
Department of Radiation Oncology
University of Michigan
Ann Arbor, Michigan

Carl S. McGill
Department of Biomedical Engineering
University of Michigan
Ann Arbor, Michigan

Qinhe Zhang
School of Mechanical Engineering
Shandong University
Jinan, Shandong
China

Haojun Zheng
Department of Precision Instrument and Mechanology
Tsinghua University
Beijing
China

KEYWORDS

Tissue Cutting, Needle Biopsy, Blade Cutting

ABSTRACT

Needle biopsy is a common medical procedure where a needle is guided into the body and used to cut and remove tissue for evaluation. The geometry of needle tip and speed of insertion are important to the efficiency of tissue cutting. This study investigates the mathematical model on the needle tip cutting edge, which is divided into several elementary cutting tools (ECT). The cutting edge is modeled as ECTs with constant inclination angle (λ). A blade oblique cutting machine was developed to test the cutting of bovine liver and phantom gel work-materials by inserting a thin sharp blade at different inclination angles. Experimentations performed reveals phenomena associated with cutting of soft tissue and tissue-like materials. Increased speeds and decreased inclination angles lead to higher cutting forces. This study also reveals that it is challenging to determine the exact location for the inception of blade cutting of soft tissue due to the large workpiece deformation.

INTRODUCTION

Biopsy is a common medical procedure where tissue is cut and removed from a specific location so that a pathologist can make an examination to detect abnormalities, such as cancer. Needle biopsy is a specific biopsy procedure where a needle and stylet (inner part of needle), as shown in Figure 1, is used to perform the biopsy operation. Needle biopsy only requires a very small incision, making it a minimally invasive procedure and therefore preferred over other biopsy techniques.

The emergence of early detection methods for cancer has increased the frequency of needle biopsy procedure. For example, in detecting prostate cancer, the most common cancer in men, the prostate specific antigen (PSA) level in the blood can be easily tested. If the PSA level is greater than 10 ng/ml, a needle biopsy is performed to confirm the presence of cancer. Efficient tissue cutting in biopsy greatly affects the accuracy of the diagnosis and comfort to the patients.

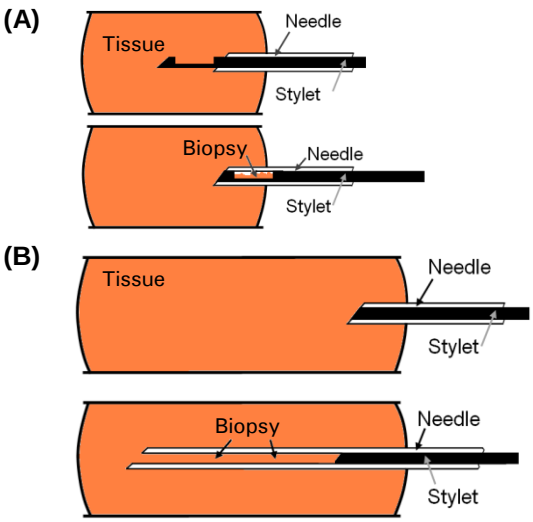

FIGURE 1. NEEDLE BIOPSY (A) TRU-CUT AND (B) END-CUT.

Needle biopsy is a tissue cutting process while the needle is used as the cutting tool. The cutting efficiency is determined by the volume of tissue acquired in each needle insertion. Using advanced needle tip geometry, optimized insertion speed, and vacuum assistance, the needle biopsy efficiency can be maximized to improve the accuracy of diagnosis and minimize trauma to the patient. Current biopsy operations commonly lack cutting efficiency, which often causes the long and painful procedures and minimizes the tissue volume that can be removed. Better needle designs that are based on an enhanced understanding of the geometric, manufacturing, and cutting mechanics aspects of the needle tip and tissue interaction would be a great contribution to enable efficient cutting of tissue in biopsy.

There are two styles of biopsy needles: the tru-cut and end-cut needle biopsy, as shown in Figure 1. The stylet is the inner rod that slides inside the needle. For tru-cut biopsy, as shown in Figure 1(A), a notch is grounded on the stylet to collect the tissue sample for biopsy. This method lacks efficiency because only a fraction of the stylet's volume can be used to collect tissue. The end-cut biopsy, as shown in Figure 1(B), uses the tip of the needle to perform the tissue cutting and the full volume of the hollow needle can collect the cut tissue (Haggarth et al., 2002). This paper explores the cutting mechanics at the tip of an end-cut biopsy needle.

The needle tip geometry, edge sharpness, as well as the cutting speed are important factors for an efficient biopsy. Tissue is a soft and strain-rate sensitive material; therefore, high speed is beneficial in fracturing and cutting the tissue. Several commercialized needle tip designs are shown in Figure 2.

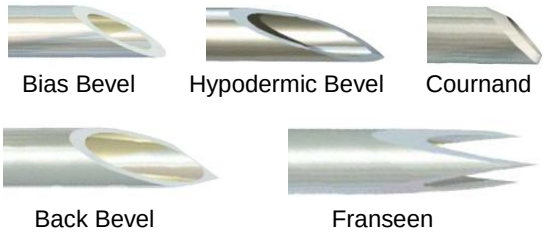

FIGURE 2. COMMON NEEDLE TIP STYLES.

Extensive research has been conducted to investigate the needle-tissue interaction upon needle insertion with the ultimate aim to build a haptic model for surgical procedures (Brett et al. 1997; Kataoka 2002; DiMaio and Salcudean 2003; Okamura et al. 2004; Hing et al. 2006; Podder et al. 2006). Podder et al. (2005) investigated the effect of needle tip geometry on force and deflection. Chanthasopeephan (2006) studied the tissue cutting force using a sharp, computer-controlled knife with the aim to build a computational model for haptic display. Dehghan et al. (2007) used an ultrasonic-based motion measurement tool to quantify the accuracy of the model for brachytherapy, a medical procedure using needles to guide radioactive seeds into position for treatment. Abolhassani et al. (2007) presents the most recent survey of needle insertion in soft tissue, including the modeling of needle insertion forces, tissue deformation, needle deflection, robot assisted needle insertion, and the effect of trajectories on tissue deformation. There is lack of fundamental study of tissue cutting between the sharp cutting edge and the soft tissue.

In this research, mathematical model of needle tip is first examined. A tissue cutting test machine is developed to insert a blade into bovine liver and phantom gel work-materials at different speeds and inclination angles. The

force and speed are recorded for cutting tests. The blade oblique cutting machine and experimental setup and results are presented.

NEEDLE TIP CUTTING EDGE AND BLADE OBLIQUE CUTTING OF TISSUE

Three styles of commonly used needle tips, one-plane bias bevel, two-plane, and three-plane (so-called Franseen), and their cutting edges are shown in Figure 3. Similar to the cutting force modeling of conventional turning and drilling processes, a force model of needle insertion into tissue can be built. The idea, as shown in Figure 3(A), is to divide the needle cutting edge into several Elementary Cutting Tool (ECT) edges. Example of ECT in one quarter of the bias bevel needle tip is shown as marked by 1 through 6. Each ECT can be modeled as a blade with straight cutting edge, which is defined by the inclination angle (λ). Experiments using thin, sharp blades with straight cutting edge of a given inclination angle can be used to study the ECT cutting of tissue, as shown in Figure 4.

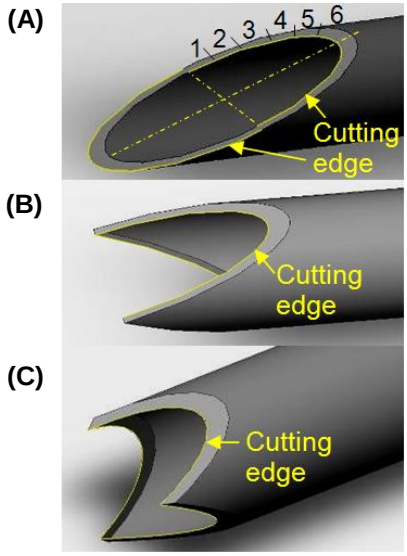

FIGURE 3. TIP AND CUTTING EDGE FOR THE (A) ONE-PLANE BIAS BEVEL (B) TWO-PLANE AND (C) THREE-PLANE FRANSEEN STYLE NEEDLE.

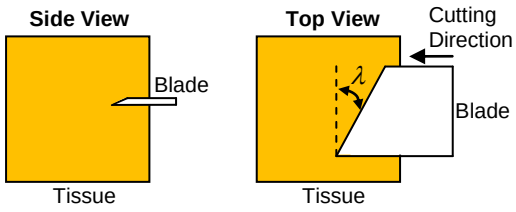

FIGURE 4. BLADE OF INCLINATION ANGLE (λ) CUTTING INTO SOFT TISSUE.

INCLINATION ANGLE OF CUTTING EDGE AT NEEDLE TIP

A geometric model of a bias bevel, two-plane, and Franseen needle cutting edge is shown in Figure 5. The cylinder radius is *r*. The angle of the plane that intersects with cylinder to create cutting edge is ξ. The angle γ is used to represent a point A on the cutting edge. At point A, the inclination angle is λ. For the bias bevel and two-plane needles, the cutting edge can be described mathematically as an ellipse. The tangent of any point on the ellipse can determine the inclination angle. An example, of the tangent at point A is illustrated in Figure 5. The angle between this tangent line and XY plane is defined as the cutting edge inclination angle, denoted as λ, at point *A*.

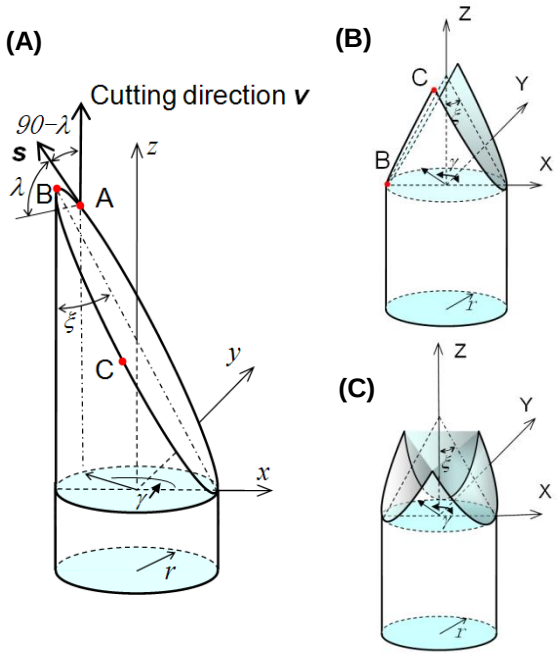

FIGURE 5. (A) BIAS BEVEL NEEDLE TIP, (B) TWO-PLANE TIP, (C) FRANSEEN TIP

As derived by Zheng et al. (2008), λ can be expressed in terms of γ and ξ as for both bias bevel and two-plane needles, by first defining the cutting edge by parametric equations in terms of γ:

$$\begin{aligned} x &= r\cos\gamma \\ y &= r\sin\gamma \\ z &= r\,(1-\cos\gamma)\cot\xi \end{aligned} \quad (1)$$

Next the tangent vector **s** can be found as: **s** = {–*r* sinγ , *r* cosγ, *r* cotξ sinγ }. The normal vector of the *xy* plane is **v** = {0, 0, 1}. The angle between **v** and **s** is the inclination angle (λ) as shown at point A on Figure 5 and found below:

$$\sin\lambda = \frac{\boldsymbol{s}\cdot\boldsymbol{v}}{\|\boldsymbol{s}\|\|\boldsymbol{v}\|} = \frac{|\cot\xi\,\sin\gamma|}{\sqrt{1+\cot^2\xi\sin^2\gamma}} \quad (2)$$

$$\lambda = \arcsin\frac{|\cot\xi\,\sin\gamma|}{\sqrt{1+\cot^2\xi\sin^2\gamma}}\ (0\le\gamma\le 2\pi) \quad (3)$$

Figure 6 shows λ vs. γ for three common needle geometries (ξ = 15, 30, and 45°). At the tip of the bias bevel needle, point B in Figure 5(A), γ = 180° and λ = 0°. This is the point where the needle first contacts the tissue and makes the cutting. As shown later in experimental results, λ = 0° is the worst cutting condition. At the side of the bias bevel needle, point C in Figure 5(A), γ = 270° and λ = 90°–ξ. This is the location with the highest λ. The tip of two-plane needle, point C in Figure 5(B), has the lowest and best cutting λ (= 90°–ξ).

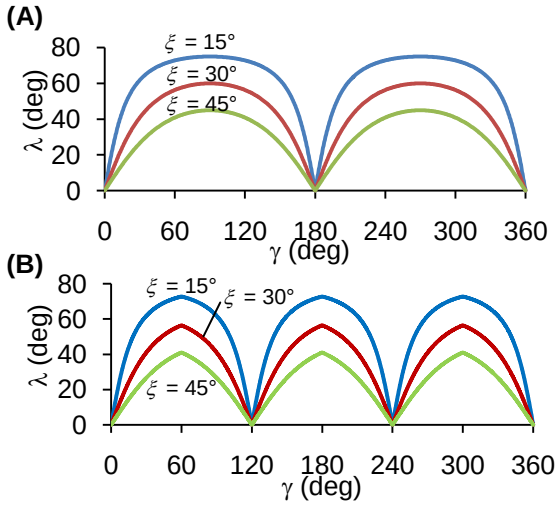

FIGURE 6. (A) BIAS BEVEL AND TWO-PLANE AND (B) FRANSEEN NEEDLES INCLINATION ANGLE.

For the three-plane Franseen needle tip geometry, the λ can be solved using Eq. (3) with $0 < \gamma < \pi/3$ and then piecewise connecting the remaining five 60° segments. Figure 6(B) shows the λ vs. γ for ξ = 15, 30, and 45°. Under the same ξ, the Franseen needle has lower λ. It also has high λ (better cutting configuration) at the needle tip.

EXPERIMENTAL SETUP

Tissue Cutting Machine

A tissue cutting machine, as shown in Figure 7, is built to study the effect of speed and inclination angle of the blade cutting into two soft tissue materials: the phantom gel (Figure 8(A)) and bovine liver (Figure 8(B)). The machine uses a pneumatic cylinder with 27 mm bore 152.4 mm stroke (Numatics SJ-557203-20) as the actuator to insert a blade into the soft workpiece at high speed. Before cutting into the soft tissue, the blade has been accelerated and reached a constant speed. This enables the cutting of tissue at a relatively constant speed. Speed of the pneumatic cylinder is controlled by varying the inlet air pressure and setting the flow control valve for the cylinder.

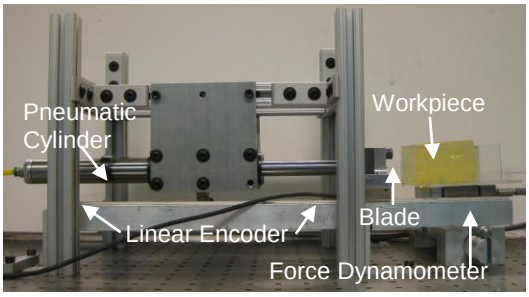

FIGURE 7. TISSUE CUTTING MACHINE WITH THE BLADE TOOL.

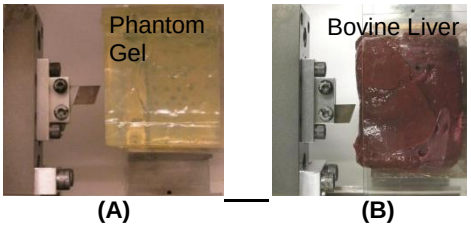

FIGURE 8. TOP VIEW OF BLADE CUTTING INTO THE WORKPIECE: (A) PHANTOM GEL AND (B) BOVINE LIVER.

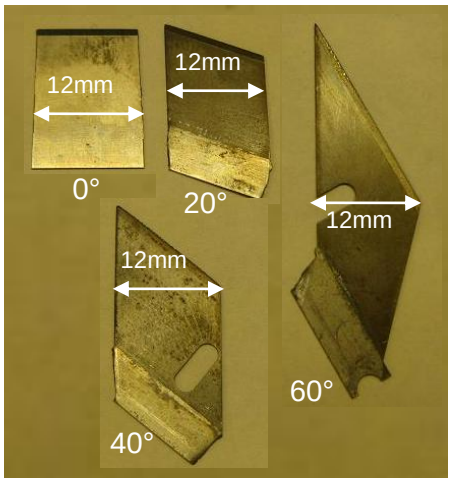

FIGURE 9. FOUR BLADES OF 0, 20, 40 and 60° INCLINATION ANGLE AND THE SAME WIDTH.

Cutting Tool

Four 0.2 mm thick single edge razor blades (made by Stanley), each having inclination angles, 0°, 20°, 40°, and 60° as shown in Figure 9, are created using the wire electrical discharge machine (EDM). Each blade has an identical width of 12 mm.

Workpiece Materials and Indentation Test

The phantom gel is produced from a mixture of 1:1 ratio of liquid plastic to plastic softener obtained from M-F Manufacturing (Ft. Worth, TX). This liquid plastic and softener material is polyvinyl chloride (PVC) modified with plastisol to increase its softness. In order to have a clear, bubble-free phantom gel, the mixture is constantly stirred while heated, before it is poured into the mold. This material was used by Sarvazyan et al. (1998) to resemble soft tissue.

A tissue indentation test, developed Egorov et al. (2008), is conducted to measure the Young's modulus for both the phantom gel and bovine liver. The tissue is compressed with a cylinder indenter, which is driven by a linear actuator. Two cylinder indenters, 4 and 8 mm in radius, are inserted at 90 mm/min speed into test sample. The indentation force and indenter displacement are measured. The Young's modulus can be calculated using the following equation (Egorov et al., 2008):

$$E = \frac{3}{\pi^2 R} \cdot \frac{F}{W} \qquad (4)$$

The Young's modulus of the bovine liver was 3.5 kPa. The phantom gel material was found to be stiffer with an average Young's modulus of 12.4 kPa.

Workpiece Fixture

During experimentation, a four-sided (both sides, beneath, and behind phantom gel) clear acrylic box, as shown in Figures 7 and 8, is used to support the phantom gel when inserting the blade. To support the bovine liver, the similar four-sided acrylic box with a clear rectangular acrylic plate placed on top (covering all sides but the blade insertion end) is used to support the liver.

Sensors and Data Acquisition System

The position of blade and the corresponding cutting force are recorded during the test. A linear optical encoder, Heidenhain Lida 277, as shown in Figure 7, measures the position of the blade. The data is recorded using data acquisition system, NI DAQPad-6015 (National Instruments; Austin, TX), at a sampling rate of 50 kHz. The force on the phantom gel and bovine liver during blade insertion is measured with a Kistler 9256A1 piezoelectric force dynamometer. The blade speed and acceleration can be calculated based on the blade displacement and time data.

BLADE DISPLACEMENT AND SPEED

An example of blade displacement for $\lambda = 60^o$ cutting of bovine liver is shown in Figure 10(A). The time and displacement are defined as 0 at the tool-workpiece contacting point. At the start (–0.09 s), the actuator is engaged and accelerated toward the workpiece. After 0.04 s, the tool reaches an almost constant speed. The blade is advanced 118 mm forward in 0.09 s before contact occurs with tissue. Upon contacting the tissue, as shown in Figure 10(B), displacement vs. time is almost a straight line ($R^2 = 0.9987$). The speed of cutting is almost constant (1.41 m/s) and acceleration is close to zero. This curve fitting method is performed to calculate the cutting speed for each test.

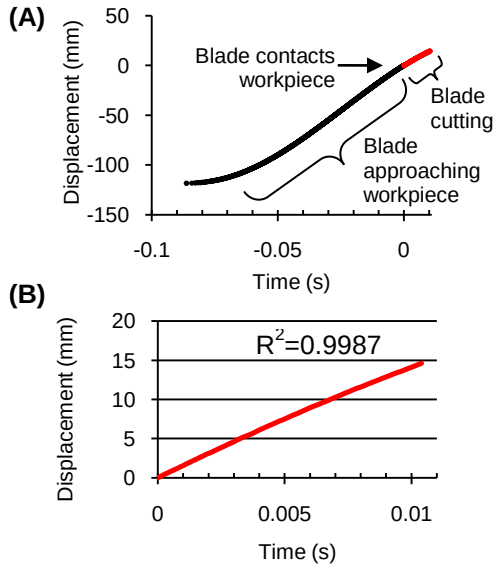

FIGURE 10. BLADE DISPLACEMENT (A) OVER THE FULL RANGE OF TRAVEL (B) DURING THE CONTACT WITH WORKPIECE.

EXPERIMENTAL PARAMETERS

Three sets of experimentation were performed, as shown in Table 1. Exp. I has four repeated tests performed at λ = 40° and about 0.2 m/s cutting speed on phantom gel to study the repeatability of a test setup. Exp. II investigates high λ (= 40 and 60°) cutting of bovine liver at two speeds (about 0.2 and 1.4 m/s). Large tissue deformation made bovine liver cutting for blade with λ less than 40° impossible. Therefore, the phantom gel with a higher Young's modulus was used to compare the performance of the varying λ. Exp. III was performed on phantom gel at four λ (0, 20, 40, and 60°) and two speeds (about 0.2 and 1.2 m/s). A total of 16 tests were performed.

EXPERIMENTAL RESULTS ON CUTTING FORCES

The four repeated tests in Exp. I show the force vs. displacement data, as shown in Figure 11, is generally repeatable. For the very soft work-material used in this study, the variation of about 25% is considered reasonable. Exp. I also shows dulling of the cutting edge is not a concern in this study.

TABLE 1: EXPERIMENTATION PARAMETERS.

	Material	Inclination Angles (deg)	Speed (m/s)	Fig. No.
Exp. I	Phantom Gel	40°	0.208	11
			0.193	
			0.218	
			0.218	
Exp. II	Bovine Liver	60°	0.202	12
			1.40	
		40°	0.200	
			1.44	
Exp. III	Phantom Gel	60°	1.20	13
			0.190	
		40°	0.185	
			1.21	
		20°	0.191	
			1.20	
		0°	0.198	
			1.24	

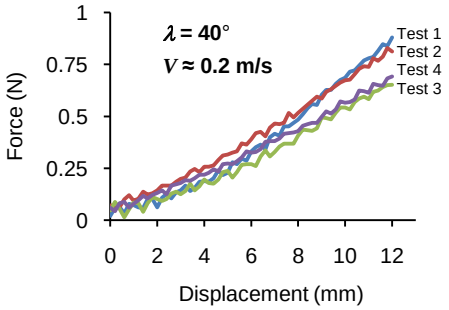

FIGURE 11. EXP. I CUTTING FORCE VS. DISPLACEMENT RESULTS OF FOUR REPEATED TESTS AND ORDER OF TEST.

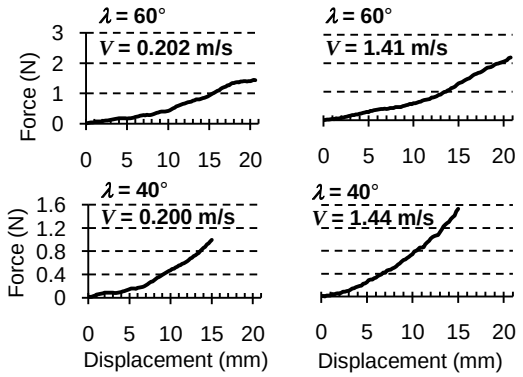

FIGURE 12. EXP. II CUTTING FORCE VS. DISPLACEMENT RESULTS.

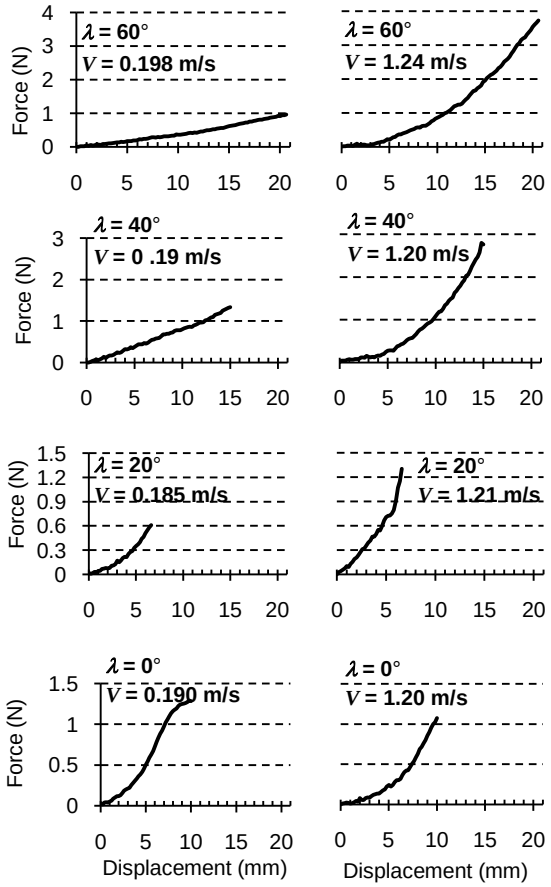

FIGURE 13. EXP. III CUTTING FORCE VS. DISPLACEMENT RESULTS.

The results in Exp. II show that higher force was produced at higher speed. This occurs because bovine liver is a strain-rate sensitive material. Friction has been shown to have a dependence on speed of needle insertion (Okamura et al. 2004). However, the frictional force between the thin blade and tissue at high speed sliding is not a well-studied area and its effect is unknown. Since bovine liver is much softer (in comparison to phantom gel), it was very difficult to vary and study the effect of λ. Furthermore, λ is varied in Exp. III for the stiffer phantom gel.

Experiment III also show that higher force was produced at higher speed under similar displacement for all tests, except at $\lambda = 0°$. At $\lambda = 0°$, the blade has almost a line contact at the start and results large workpiece deformation and very sharp increase in cutting force. A higher λ is observed to lead to lower cutting forces. This can be attributed to the fact that the sharper angle requires less force to break the polymer chains in the phantom gel.

The cutting force vs. displace curve can be used to identify the time when needle penetrates into the soft work-material. For example, the bovine liver experiment that was performed at 0.244 m/s with $\lambda = 40°$, Figure 14, shows two force regions during the blade insertion. The transition point is likely when the blade is penetrating into the tissue. For other tests, this blade penetrating point is not obvious and difficult to accurately determine. It is a future research topic.

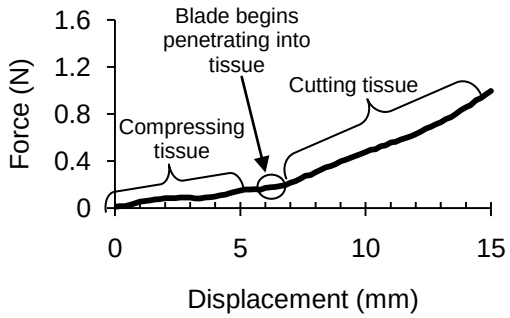

FIGURE 14. TWO DISTINCT REGIONS (COMPRESSION AND CUTTING) AT LOW CUTTTING SPEED.

CONCLUSIONS

A blade oblique cutting machine was developed to investigate the effect of inclination angle and speed on cutting soft bovine liver and phantom gel. A mathematical model was examined to find the inclination angle of ECT on cutting edges of three needle styles (bias bevel, two-plane, and Franseen). Experimental results showed that higher speed produced higher force for both work-materials. High inclination angle was benefit for cutting tissue. Observations in this research could lead to the design of new, novel needle tip geometry and needle insertion speed for more efficient biopsy.

ACKNOWLEDGEMENTS

This research work is sponsored by the National Science Foundation (NSF) Award CMMI#0825795 and supported by the University of Michigan Radiation Oncology Department.

REFERENCES

Abolhassani, N., R. Patel, and M. Moallem. Needle insertion into soft tissue: A survey, *Medical Engineering & Physics*, 29, 413-431, 2007.

Brett, P.N., T.J. Parker, A.J. Harrison, T.A. Thomas, and A. Carr. Simulation of resistance forces acting on surgical needles, *Proc. Instn Mech Engrs*, 211, 335-347, 1997.

Chanthasopeephan, T. Characterization of Soft Tissue Cutting for Haptic Display: Experiments and Computational Models, *PhD Dissertation*, Drexel University, 2006.

Dehghan, E., X. Wen, R. Zahiri-Azar, M. Marchal, and S.E. Salcudean. Modeling of Needle-Tissue Interaction Using Ultrasound-Based Motion Estimation, In: *MICCAI 2007*, Part I, LNCS 4791, 709–716, 2007.

DiMaio, S.P. and S.E. Salcudean. Needle insertion modeling and simulation, *IEEE Trans. on Robot Autom.: Special Issue on Medical Robotics*, 19, 864–875, 2003.

Egorov, V., S. Tsyuryupa, S. Kanilo, M. Kogit, and A. Sarvazyan. Soft Tissue Elastometer. *Medical Engineering & Physics*, 30, 206-212, 2008.

Haggarth, I., P. Ekman, and L. Egevad. A New Core-Biopsy Instrument with an End-Cut Technique Provides Prostate Biopsies with Increase Tissue Yield. *BJU International*. 90, 51-55, 2002.

Hing, J.T., A.D. Brooks, and J.P. Desai. Reality-based needle insertion simulation for haptic feedback in prostate brachytherapy, In: *Proc. IEEE ICRA*, 619–624, 2006.

Kataoka, H., T. Washio, K. Chinzei, K. Mizuhara, C. Simone, and A.M. Okamur. Measurement of the Tip and Friction Force Acting on a Needle during Penetration, In: *Proceedings of the Fifth International Conference on Medical Image Computing and Computer Assisted Intervention MICCAI*, 216-223, 2002.

Okamura, A.M., C. Simone, and M.D. O'Leary. Force modeling for needle insertion into soft tissue, *IEEE Transactions on Biomedical Engineering*, 51, 1707-1716, 2004.

Podder, T.K., D.P. Clark, J. Sherman, D. Fuller, E.M. Messing, D.J. Rubens, J.G. Strang, Y.D. Zhang, W. O'Dell, W.S. Ng, and Y. Yu. Effects of tip geometry of surgical needles: an assessment of force and deflection, In: *The 3rd European Medical and Biological Engineering Conference EMBEC'05, Prague, Czech Republic*, November 20-25, 2005.

Podder, T.K., J. Sherman, E. Messing, D. Rubens, D. Fuller, J. Strang, R. Brasacchio, and Y. Yu. Needle insertion force estimation model using procedure-specific and patient-specific criteria, In: *Proc. IEEE EMBS Int. Conf*, 555–558, 2006.

Sarvazyan, T., V. Stolarsky, B. Fishman, and A. Sarvazyan. Development of Mechanical models or Breast and Prostate with Palpable Nodules. *International Conference of the IEEE Engineering in Medicine and Biology Society*. Vol. 20, No 2, 1998.

Zheng, H., Q. Zhang, J. Moore, J. Schwartza, C. McGill, P.W. McLaughlin, and A.J. Shih. Biopsy Needle Tissue Cutting Analysis. *Proceedings of the 8th International Conference on Frontiers of Design and Manufacturing*, Tianjin, China. Sept.23-26, 2008.